J. LI, C. F. ZHANG, R. M. YIN, W. H. ZHANG

ISSN 0543-5846
METABK 57(4) 231-234 (2018)
UDC – UDK 62.001.57:666.3/.7:620.18:536.421-622.785=111

MONTE CARLO SIMULATION OF ANISOTROPIC GROWTH OF GRAINS DURING LIQUID PHASE SINTERING FOR CERAMICS

Received – Primljeno: 2018-03-16
Accepted – Prihvaćeno: 2018-06-15
Original Scientific Paper – Izvorni znanstveni rad

An improved two-dimensional Q-State Monte Carlo Potts model for describing anisotropic growth of grains of ceramics is established. The sintering additives, pores, and second-phase particles introduced into the ceramic matrix have been fully considered in the new algorithm. Using this model, the influence of the second-phase particles on the microstructural evolution of ceramics with elongated grain morphology are investigated. Results show that the addition of the second-phase particles obviously hinders the anisotropic growth of grains, thereby resulting in a slightly decreased average grain size and grain growth exponent. The preliminary investigation indicates that the simulation results are in good agreement with the existing sintering kinetic theory.

Keywords: Monte carlo simulation, ceramic, microstructure, anisotropic growth, liquid phase sintering

INTRODUCTION

The in situ toughened ceramics have excellent mechanical properties at room and high temperature [1]. Increasing evidence has been observed on the introduction of second-phase particles to the in situ toughened ceramic matrix as enhanced components to achieve a synergistic toughening effect of the two mechanisms [2]. However, the anisotropic growth of grains during liquid phase sintering (LPS) determines the final microstructural morphology of the self-toughening ceramic material, and the addition of the second-phase particles complicates the formation of the microstructure. Therefore, investigating the microstructural evolution of ceramic materials by modeling and numerical simulation of LPS is a significant task.

Recently, the Q-State Monte Carlo Potts (QSMCP) model has been expanded to investigate the grain growth mechanisms of two-phase ceramic material. For example, Fang et al. [3] proposed a two-dimensional (2D) Monte Carlo Potts(MCP) model for isotropic grain growth for two-phase ceramic materials, and the effect of two-phase size on the growth rate of matrix phase was discussed in detail. However, the presence of pores and liquid additives were not considered. Also, the MCP model was widely applied to simulate the anisotropic growth of grains. Yang et al. [4] first established a Monte Carlo model to investigate the anisotropic grain growth of single-phase ceramics and found that the anisotropy of grain boundary energies can significantly affect the anisotropy microstructure. Brown et al. [5] extended Yang's model to simulate the pore migration and vacancy annihilation of ceramics with anisotropic grains. Currently, reports on the microstructural evolution of ceramic materials co-toughened by self-toughening and diffusion toughening of second-phase particles have been few.

J. Li (133501020@csu.edu.cn), C. F. Zhang, W. H. Zhang, School of Metallurgy and Environment, Central South University, Changsha, China. R. M. Yin, College of Metallurgical Engineering, Hunan University of Technology, Zhuzhou, China

SIMULATION MODEL

The model consists of a QSMCP model, a liquid phase growth model, and a pore migration and vacancy annihilation model.

QSMCP model

The continuum microstructure is mapped onto a suite of 2D discrete hexagonal lattice sites. In the QSMCP model, each lattice site possesses two states (*P* and *Q*), where *Q* is the maximum value for the grain orientation and *P* represents the type of the site, to distinguish each other from the coexistence of the matrix phase 1, second particle phase 2, liquid phase 3, and gas phase 4 in the material system. For the matrix phase 1, the value of *P* is 1 and the orientation indices of matrix phase 1 are randomly assigned in the range of 1 to *q*; adjacent grain lattices with the same orientation form crystal grains, and adjacent grain lattices with different orientations form grain boundaries. For the second particle phase 2, the value of *P* is 2 and the value of *Q* is -1. For the liquid phase 3, the value of *Q* is -2. For the gas phase 4, the value of *Q* is -3 [6]. The total energy of the system and grain boundary energy of each phase can be expressed as follows:

$$E_{Tol} = E_{11} + E_{22} + E_{12} + E_{13} + E_{23} + E_{14} + E_{24} + E_{34} \quad (1)$$

$$E_{11} = J_{11}\sum_{i=0}^{N_1}\sum_{j=0}^{n_1}\left[1-\delta\left(q_i, q_j\right)\right] \quad (2)$$

$$E_{22} = J_{22}\sum_{i=0}^{N_2}\sum_{j=0}^{n_2}\left[1-\delta\left(q_i, q_j\right)\right] \quad (3)$$

$$E_{12} = J_{12}\sum_{i=0}^{N_3}\sum_{j=0}^{n_3}\left[1-\delta\left(q_i, q_j\right)\right] \quad (4)$$

$$E_{13} = J_{13}\sum_{i=0}^{N_1}\sum_{j=0}^{n_4}\left[1-\delta\left(q_i, q_j\right)\right] \quad (5)$$

$$E_{23} = J_{23}\sum_{i=0}^{N_2}\sum_{j=0}^{n_4}\left[1-\delta\left(q_i, q_j\right)\right] \quad (6)$$

$$E_{14} = J_{14}\sum_{i=0}^{N_1}\sum_{j=0}^{n_5}\left[1-\delta\left(q_i, q_j\right)\right] \quad (7)$$

$$E_{24} = J_{24}\sum_{i=0}^{N_2}\sum_{j=0}^{n_5}\left[1-\delta\left(q_i, q_j\right)\right] \quad (8)$$

$$E_{34} = J_{34}\sum_{i=0}^{n_4}\sum_{j=0}^{n_5}\left[1-\delta\left(q_i, q_j\right)\right] \quad (9)$$

$$J_{ij} = J_\theta\left(q_i\right) + J_\theta\left(q_j\right) - J_b \quad (10)$$

Where E_{Tol} is the total energy, E_{11} is the grain boundary energy of the neighboring anisotropic grain (phase 1) sites, E_{22} is the grain boundary energy of the neighboring second-phase grain (phase 2) sites, E_{12} is the grain boundary energy of the neighboring phase 1 and phase 2, E_{13} is the grain boundary energy of the neighboring phase 1 and phase 3, E_{23} is the grain boundary energy of the neighboring phase 2 and phase 3, E_{14} is the grain boundary energy of the neighboring phase 1 and phase 4, E_{24} is the grain boundary energy of the neighboring phase 2 and phase 4, and E_{34} is the grain boundary energy of the neighboring phase 3 and phase 4. N_1 is the site number of the matrix phase 1, N_2 is the site number of the second particle phase 2, N_3 has a smaller value than N_1 and N_2. n_1 is the phase 1 site number around one specific site of phase 1 (≤6), n_2 is the phase 2 site number around one specific site of phase 2 (≤6), n_3 is the phase 2 site number around one specific site of phase 1 when $N_3 = N_1$; otherwise, it is the phase 1 site number around one specific site of phase 2 when $N_3 = N_2$(≤6), n_4 is the phase 1 site number around one specific site of phase 3 (≤6), and n_5 is the phase 1 site number around one specific site of phase 4 (≤6). $\delta(q_i, q_j)$ is the Kronecker function($\delta(q_i, q_j)$=1 when q_i=q_j, $\delta(q_i, q_j)$=0 when $q_i \neq q_j$). J_θ (q_i) is the surface energy of q_i at the plane normal to the axisθ (where θ=*0*, π/3, or 2π/3), J_b is the grain boundary binding energy which is equal to 0,3, and $J_\theta(q_j)$ is calculated by Wulff plot in detail according to the literature [4].

In this study, grain growth is achieved by a lattice reorientation attempt. The energy change before and after reorientation of the system is calculated by equation (1), and equation (11) is used to determine the acceptance of the orientation attempt.

$$p = \begin{cases} \exp\left(-\dfrac{\Delta E}{k_B T}\right) & \Delta E > 0 \\ 1 & \Delta E \le 0 \end{cases} \quad (11)$$

Where ΔE is the energy difference before and after reorientation, k_B is the Boltzmann constant, and T is the absolute temperature.

Dissolution-diffusion-precipitation model

For the liquid phase lattice, exchange attempts are made in the following three states for the neighboring solid-phase lattice A and liquid-phase lattice B [7], as shown in Figure 1.

Pore migration and vacancy annihilation model

The pore lattice adjacent to the grain boundary and the solid-phase lattice adjacent to the selected pore lattice are randomly selected. The aforementioned two selected lattices are exchanged, and then a new orientation that satisfies minimizing the system energy is given to the solid-phase lattice after the exchange. The energy change (ΔE) after the aforementioned exchange attempts is calculated, and then the probability of accepting the exchange attempt is calculated according to equation (11), which is used to simulate the pore diffusion process [8]. For the vacancies on the grain boundaries, the vacancy annihilation method is used to simulate the pore discharge process [8].

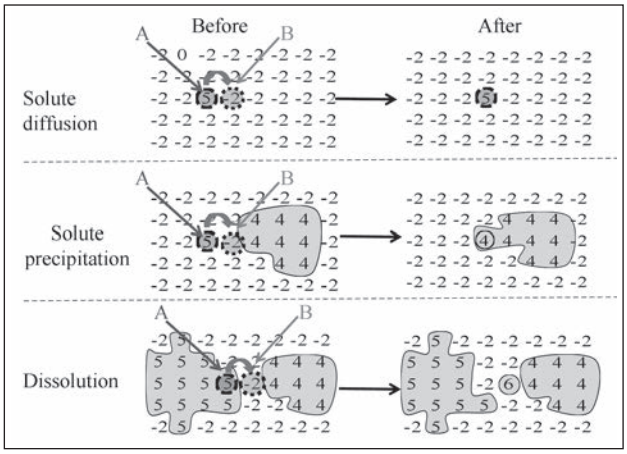

Figure 1 Schematic of state exchange attempt for neighboring solid and liquid lattice

Simulation conditions

This model is implemented by using C# programming language. The simulation domain is performed in 256 × 256 hexagon sites. The maximum value for the grain orientation (Q) is 60. The edge length of the hexagonal site is 0,6 μm. The vacancy diffusion rate is 0,3 and K_bT is 0,7. The specific grain boundary energy ratio is J_{11}: J_{12}:J_{22} J_{13}:J_{23}:J_{14} J_{24}:J_{34} = $J_{11}(q_i, q_j)$:1:3:1:1:1:1:1.

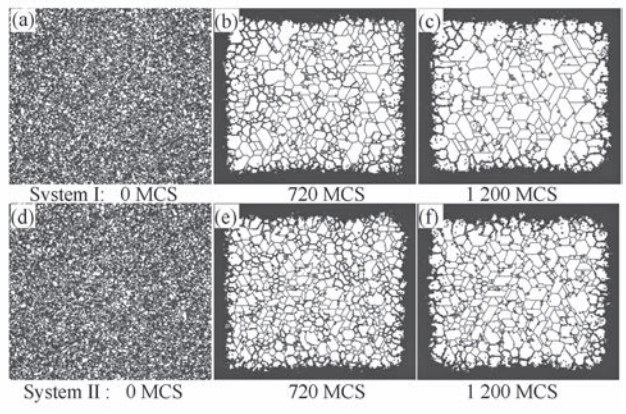

Figure 2 Microstructure evolution

The simulation time is represented by the number of MCS, and the simulation time is 1 200 MCS for the Systems I and II, where the initial grains size is 2,7 μm, the porosity is 30 vol %, and the liquid phase is 4 vol %. There is no second-phase particle addition in System I, but there is 3 vol % second-phase particles with size of 1,0 μm added in System II. The simulation data are the average results of the 15 independent simulations to ensure the accuracy of statistical results.

RESULTS AND DISCUSSION

Microstructure evolution

Figure 2 shows the temporal microstructure evolution for grain growth at the same temperature for different MCS, where the white regions indicate the matrix phase, the red regions indicate the sintering liquid additives, the blue regions indicate the second-phase particles and the dark regions indicate the grain boundary and pores. From Figures 2(a) to 2(c), a large number of stomatal series channels are formed in the simulation region, which promotes the stomata move from the internal simulation zone to the boundary, thereby achieving the densification of materials. In addition, grain growth and densification are performed simultaneously, and the grain anisotropy characteristics become increasingly obvious with the increase in simulation time. However, grain growth becomes relatively slow due to the hindrance of pores [5].

As shown in Figure 2(d), the second-phase particles can cause grain aggregations during powder mixing processes. As shown in Figure 2(e), the grain size of the matrix phase around the pores is generally larger than that around the second-phase particles, thereby indicating that the effect of the second-phase particles on the grain growth retardation is stronger than that of the pores. This condition is due to the pore migration. However, the second-phase particles undergo difficult migration because no dissolution precipitation occurs during the sintering process. Figure 2(f) shows that grains are almost elongated in shape, and most of the second-phase particles migrate from the grain boundary to the triple point. The grain size of the matrix phase around the second-phase particles is obviously reduced, but the

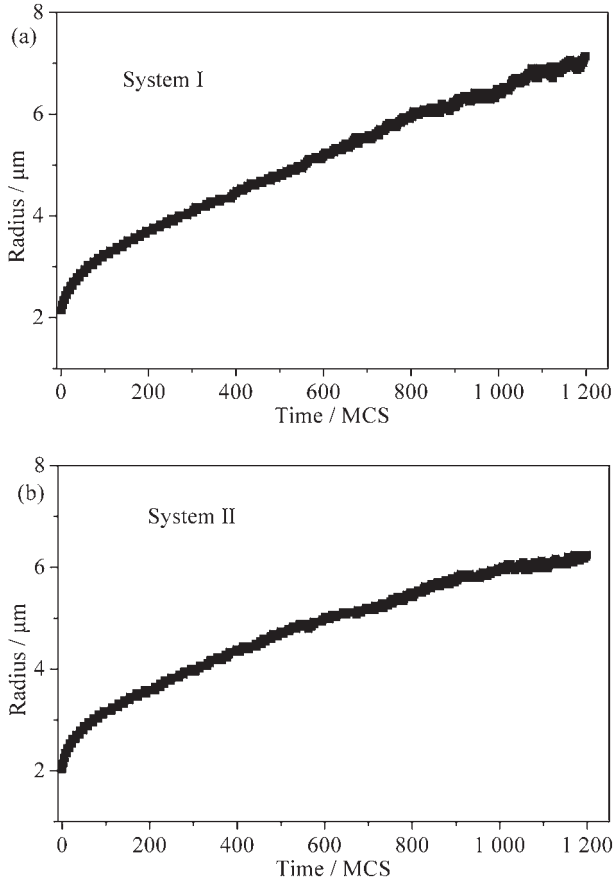

Figure 3 Relation curve between average grain radius and simulation times

grain growth rate is faster in the region adjacent to the matrix phase. This condition indicates that the second-phase particles have a strong pinning effect and the second-phase particles significantly inhibit the grain anisotropic growth.

Grain size and grain growth exponent

The grain growth can be described by the average grain radius increases during the simulation process, and the average grain size can be calculated by equation (12) as follows [3]:

$$\overline{R}_{\text{avg}} = \sqrt{\frac{N_{Tol} \cdot A_0}{N_{Grain}}} \tag{12}$$

Where $\overline{R}_{\text{avg}}$ is the average grain radius, A_0 is the lattice area, and N_{Tol} and N_{Grain} are the total number of site and grain in the simulation region, respectively.

The relation curves between average grain radius and simulation times (MCS) of systems I and II are shown in Figure 3. As shown in Figure 3, the average grain size increases with simulation time, but due to the addition of the second phase particles it is significantly reduced from 7,38 μm to 5,69 μm after simulation with 1 200 MCS.

Figure 4 shows the grain size distribution of the microstructure at 1 200 MCS. It can be found that the grain size is obviously reduced due to the addition of the second phase particles. The small size of the grains in the

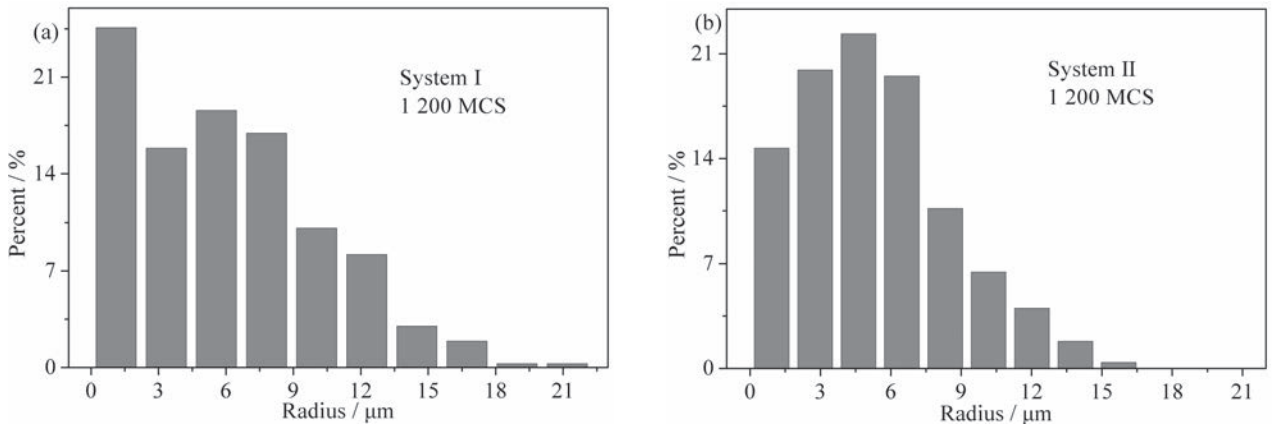

Figure 4 Grain size distribution, a) Sistem I, b) Sistem II

range of 0 μm to 2,25 μm is observed to account for the highest proportion of 24,5 % for system I, and the relatively large grain sizes in the range of 3,5 μm to 4,5 μm are observed to account for the highest proportion at 22,5 % for system II.

The grain growth rate can be characterized by the grain growth exponent, which can be calculated by the power law relationship for grain growth kinetics [3].

$$\overline{R} = (kt)^n \tag{13}$$

Where n is the grain growth exponent, $\overline{R}$ is the average grain size at time t, and k is a constant.

The grain growth exponents at different times are shown in Table 1. Table 1 presents a certain degree of reduction for the grain growth exponents, which reduces from 0,28 for Figure 2(c) to 0,24 for Figure 2(f) because the second-phase particles pin the matrix phase during the grain growth, which is close to the theoretical growth exponent [7].

Table 1 **Grain growth exponent**

System	Time / MCS	Average grain radius / μm	Grain growth exponent
I	720	5,13	0,23
	1 200	7,38	0,28
II	720	4,91	0,20
	1 200	5,69	0,24

CONCLUSIONS

An improved 2D QSMCP model to describe the anisotropic growth of grains of self-toughening ceramic materials has been established. This model is developed to investigate the four-phase systems. The sintering mechanisms of anisotropic grain growth, pore migration and vacancy annihilation, LPS aids and the second-phase particles were incorporated into the ceramic systems for simulation. The results show that the model can successfully simulate the microstructural evolution of ceramic materials with anisotropic grain morphology during LPS. The preliminary investigation indicates that the simulation results are in good agreement with the existing sintering kinetic theory.

Acknowledgements

This work is financially supported by the National Natural Science Foundation of China (No. 51574120).

RERERENCES

[1] X. Sun, K. Sun, A. Li, M. Du, Y. Zhao. In situ synthesis of FeSi particle toughening Si_3N_4 composite, International Journal of Refractory Metals and Hard Materials 37(2013), 142-147.

[2] H. Hu, Y. Zeng, Y. Xia, D. Yao, K. Zuo, J. Günster, J.G. Heinrich. Rapid fabrication of porous Si_3N_4/SiC ceramics via nitridation of silicon powder with ZrO_2 as catalyst, Ceramics International 40(2014), 7579-7582.

[3] B. Fang, C.Z. Huang, H.L. Liu, C.H. Xu, S. Sun. Monte Carlo simulation of grain-microstructure evolution in two-phase ceramic tool materials, Journal of Materials Processing Technology 209(2009), 4568-4572.

[4] W. Yang, L.Q. Chen, G.L. Messing. Computer simulation of anisotropic grain growth, Materials Science & Engineering A 195(1995), 179-187.

[5] G. Brown, R.A. Levine, V. Tikare, E. Olevsky. Meso-scale Monte Carlo Sintering with Anisotropic Grain Growth, Advances in Sintering Science and Technology: Ceramic Transactions (2010), 101-111.

[6] J.W. Lee. Monte Carlo Simulation of Densification during Liquid-Phase Sintering, Journal of the Korean Ceramic Society 53(2016)3, 288-294.

[7] X.Y. Zhang, S.S. Liu, Y.X. Bao, X.B. Li, K.C. Zhou. Monte Carlo simulation for precipitation and growth behaviors in supersaturated liquid, Chinese Journal of Nonferrous Metals 23(2013), 3202-3210.

[8] M. Braginsky, V. Tikare, E. Olevsky. Numerical simulation of solid state sintering, International Journal of Solids and Structures 42(2005), 621-636.

Note: The professional translator for the English language is doctor J. D. Huang, Nanchang, China.